

# SPring-8 LEPS2 beamline: A facility to produce a multi-GeV photon beam via laser Compton scattering

N. Muramatsu<sup>a</sup>, M. Yosoi<sup>b</sup>, T. Yorita<sup>b</sup>, Y. Ohashi<sup>b</sup>, J.K. Ahn<sup>c</sup>, S. Ajimura<sup>b</sup>, Y. Asano<sup>d</sup>, W.C. Chang<sup>e</sup>, J.Y. Chen<sup>f</sup>, S. Daté<sup>b</sup>, T. Gogami<sup>g</sup>, H. Hamano<sup>b</sup>, T. Hashimoto<sup>b</sup>, T. Hiraiwa<sup>h</sup>, T. Hotta<sup>b</sup>, T. Ishikawa<sup>a</sup>, Y. Kasamatsu<sup>b</sup>, H. Katsuragawa<sup>b</sup>, R. Kobayakawa<sup>b</sup>, H. Kohri<sup>b</sup>, S. Masumoto<sup>i</sup>, Y. Matsumura<sup>a</sup>, M. Miyabe<sup>a</sup>, K. Mizutani<sup>j</sup>, Y. Morino<sup>k</sup>, T. Nakano<sup>b</sup>, T. Nam<sup>b</sup>, M. Niyama<sup>l</sup>, Y. Nozawa<sup>m</sup>, H. Ohkuma<sup>b,n</sup>, H. Ohnishi<sup>a</sup>, T. Ohta<sup>m</sup>, M. Oishi<sup>o</sup>, K. Ozawa<sup>k,i</sup>, S.Y. Ryu<sup>b</sup>, Y. Sada<sup>a</sup>, H. Saito<sup>a</sup>, T. Shibukawa<sup>i</sup>, H. Shimizu<sup>a</sup>, R. Shirai<sup>a</sup>, M. Shoji<sup>o</sup>, M. Sumihama<sup>p,b</sup>, S. Suzuki<sup>o</sup>, S. Tanaka<sup>b</sup>, Y. Taniuchi<sup>o</sup>, A. O. Tokiyasu<sup>a</sup>, N. Tomida<sup>b</sup>, Y. Tsuchikawa<sup>q</sup>, K. Watanabe<sup>b</sup>, C.J. Yoon<sup>b</sup>, C. Yoshida<sup>a</sup>

<sup>a</sup>Research Center for Electron Photon Science, Tohoku University, Sendai, Miyagi 982-0826, Japan

<sup>b</sup>Research Center for Nuclear Physics, Osaka University, Ibaraki, Osaka 567-0047, Japan

<sup>c</sup>Department of Physics, Korea University, Seoul 02841, Republic of Korea

<sup>d</sup>XFEL Project Head Office, RIKEN, Sayo, Hyogo 679-5143, Japan

<sup>e</sup>Institute of Physics, Academia Sinica, Taipei 11529, Taiwan

<sup>f</sup>National Synchrotron Radiation Research Center, Hsinchu 30076, Taiwan

<sup>g</sup>Department of Physics, Kyoto University, Kyoto 606-8502, Japan

<sup>h</sup>RIKEN SPring-8 Center, Sayo, Hyogo 679-5148, Japan

<sup>i</sup>Department of Physics, University of Tokyo, Tokyo 113-0033, Japan

<sup>j</sup>Thomas Jefferson National Accelerator Facility, Newport News, Virginia 23606, USA

<sup>k</sup>Institute of Particle and Nuclear Studies, High Energy Accelerator Research Organization (KEK), Tsukuba, Ibaraki 305-0801, Japan

<sup>l</sup>Department of Physics, Kyoto Sangyo University, Kyoto 603-8555, Japan

<sup>m</sup>Department of Radiology, The University of Tokyo Hospital, Tokyo 113-8655, Japan

<sup>n</sup>Aichi Synchrotron Radiation Center, Seto, Aichi 489-0965, Japan

<sup>o</sup>Japan Synchrotron Radiation Research Institute (SPring-8), Sayo, Hyogo 679-5198, Japan

<sup>p</sup>Department of Education, Gifu University, Gifu 501-1193, Japan

<sup>q</sup>J-PARC Center, Japan Atomic Energy Agency, Tokai, Ibaraki 319-1195, Japan

---

## Abstract

We have constructed a new laser-Compton-scattering facility, called the LEPS2 beamline, at the 8-GeV electron storage ring, SPring-8. This facility provides a linearly polarized photon beam in a tagged energy range of 1.3–2.4 GeV. Thanks to a small divergence of the low-emittance storage-ring electrons, the tagged photon beam has a size ( $\sigma$ ) suppressed to about 4 mm even after it travels about 130 m to the experimental building that is independent of the storage ring building and contains large detector systems. This beamline is designed to achieve a photon beam intensity higher than that of the first laser-Compton-scattering beamline at SPring-8 by adopting the simultaneous injection of up to four high-power laser beams and increasing a transmittance for the long photon-beam path up to about 77%. The new beamline is under operation for hadron photoproduction experiments.

**Keywords:** high energy photon beams, laser Compton scattering, linear polarization, hadron photoproduction

---

## 1. Introduction

Photon beams in the energy range from a few hundred MeV to several GeV are useful tools to investigate the structures and properties of hadrons, which can be produced by the reaction of a photon with a target nucleon or nucleus (hadron photoproduction). In particular, photon beams with a few GeV energies are suitable for hadron studies in the strange sector. As a distinct feature, photons can be polarized linearly or circularly. This feature is effective to obtain the spin and parity information of hadrons in photoproduction reactions. Currently, high-energy photon beams for hadron photoproduction experiments are generated by laser Compton scattering or bremsstrahlung at several facilities in the world. So far, facilities based on the laser Compton scattering were realized at SPring-8 (LEPS) [1, 2], ESRF (GRAAL) [3], and BNL (LEGS) [4]. However, only the LEPS2 beamline at SPring-8, described in this article, is now under operation as the laser Compton scattering facility. On the other hand, the high-energy photon-beam production by bremsstrahlung has been achieved at JLab [5], ELSA [6], MAMI [7], ELPH [8, 9] etc.

For laser Compton scattering, high-intensity laser light is injected into a high-energy electron storage ring so that photons should be backscattered over a very narrow angular region [10, 11, 12]. At this scattering, the energy of a photon is greatly amplified by receiving a large fraction of the energy of an electron. While the beam production by bremsstrahlung requires a dedicated electron accelerator, the laser Compton scattering facility has an advantage of low-cost operation at one of many beamlines in an electron storage ring. In addition, demands for the electron storage rings are increasing as synchrotron radiation sources for material, earth, life sciences etc. Therefore, the laser Compton scattering is utilized not only for hadron photoproduction experiments in the GeV energy region but also for various researches and applications with MeV photon beams [13, 14, 15]. The energy spectrum of a photon beam obtained by laser Compton scattering has a continuously spread shape with a maximum at the Compton edge, whereas the intensity of bremsstrahlung

decreases in inverse proportion to the photon energy. The photon beam production by laser Compton scattering significantly reduces a low-energy component, which cannot be tagged in the energy measurement and contributes as experimental backgrounds.

Laser light is almost 100% linearly polarized, and it is easy to control the direction of a linear polarization or make circular polarization by using a waveplate (retarder) [16]. The polarization state of the laser light can be transferred to the photon beam by Compton scattering in a wide energy range. For both linearly and circularly polarized photon beams, the degree of polarization increases as the energy goes up to the Compton edge [17, 18]. On the other hand, a linearly polarized component of the bremsstrahlung beam is generated in a relatively narrow energy range (coherent bremsstrahlung [19]), and the polarization decreases as this range is adjusted to the higher energy side. A high-energy coherent bremsstrahlung beam with high linear-polarization is only achieved by increasing the energy of an electron beam, as recently done in JLab for the photon beam energies around 9 GeV [20]. In the energy range from approximately 2 to several GeV, there are no bremsstrahlung facilities providing high linear-polarization for a photon beam. Instead, the laser Compton scattering beamlines at SPring-8 have generated a highly linear-polarized photon beam in the energy range up to the Compton edge, exceeding 2 GeV. For the production of a circularly polarized photon beam, a highly polarized electron beam is necessary at bremsstrahlung facilities [21] with a high cost. Whereas, the circular polarization of a laser-Compton-scattering beam can be obtained only by the optical control of incident laser light.

The LEPS beamline (BL33LEP) has been operated since 1999 as the first laser Compton scattering facility at SPring-8, which is a storage ring with an electron energy of 7.975 GeV. The photon beam energy at this beamline is the world's highest among the facilities adopting laser Compton scattering. When the energy of incident laser light, the energy of an electron storage ring, and the rest mass of an electron are denoted by  $k$ ,  $E_e$ , and  $m_e$ , respectively, the maximum energy of a photon beam via laser Comp-

ton scattering ( $E_\gamma^{\max}$ ) is written as

$$E_\gamma^{\max} \simeq \frac{4E_e^2 k}{m_e^2 c^4 + 4E_e k}. \quad (1)$$

At the LEPS beamline, ultraviolet (UV) laser light with a wavelength of 355 nm ( $k = 3.49$  eV) is injected into SPring-8 to produce a photon beam in the energy range up to  $E_\gamma^{\max} = 2.39$  GeV [1]. The intensity of this photon beam (the counting rate of photons that are tagged and reach a detector system for hadron photoproduction experiments) has been about  $10^6$  s<sup>-1</sup> with the laser output power of 8 W. The stabilization and maximization of a Compton scattering rate have been realized by the top-up operation that constantly refills electrons to the storage ring up to 100 mA [22]. Nevertheless, the obtained beam intensity is still an order of magnitude lower than that of the bremsstrahlung facilities. In order to get a higher photon-beam intensity without accelerator upgrades, it is necessary to increase the total power of incident laser light and the photon-beam transmittance over the entire beamline. The incident power can be improved by operating multiple high-power UV lasers simultaneously, and the transmittance goes up by the reduction of beamline materials.

For the photoproduction of heavier hadrons, it is also an important issue to further raise the photon beam energy while attaining a reasonable beam intensity. Advances in the laser technology have made it possible to shorten the wavelength of incident light in Compton scattering for the production of a higher-energy photon beam. The LEPS beamline has succeeded in generating a photon beam up to the energy  $E_\gamma^{\max} = 2.89$  GeV by using deep-UV lasers with a wavelength of 266 nm ( $k = 4.66$  eV). However, the output power of an existing deep-UV laser is about an order of magnitude lower than that of the UV laser with a wavelength of 355 nm. As a result, the photon beam intensity achieved by the injection of deep-UV lasers has been limited to about  $10^5$  s<sup>-1</sup>. It is indispensable to develop high-power lasers also for the deep-UV wavelength and construct a system for the simultaneous injection of them. These developments in the laser injection is essential to obtain

a higher-energy photon beam in future because the electron beam energies of new storage rings tend to be reduced below the SPring-8 energy in order to aim for higher-brilliance synchrotron radiation.

For the purpose to solve the above problems of the photon beam intensity and energy, the LEPS2 beamline (BL31LEP) has been newly constructed as the second laser Compton scattering facility at SPring-8. Its operation has started in 2013 [23]. The LEPS2 beamline is designed to allow the injection of up to four laser beams with either of the UV (355 nm) or deep-UV (266 nm) wavelength. New high-power lasers are also being introduced step by step. In addition, the LEPS2 beamline has succeeded in taking a sufficient space to construct large and complex detector-systems for hadron photoproduction experiments. So far, the LEPS beamline has been built in the experimental hall common to many other beamlines, and the LEPS experimental setup has been made compact by specializing in the detection of charged particles that are produced at extremely forward angles [18, 24]. In the case of the LEPS2 beamline, experimental setups that can detect both charged and neutral particles over almost all solid angles have been assembled in a large space inside the LEPS2 experimental building. This building is independent of the storage ring building housing the common experimental hall together. Two types of large-acceptance detector systems with different characteristics are installed into the LEPS2 experimental building, and alternately operated according to experimental programs. The construction of the LEPS2 experimental building was possible because a spread of the photon beam is well suppressed thanks to a small divergence of the electron beam in the LEPS2 beamline.

This article describes the details of the LEPS2 beamline facility together with the design concepts. In addition, the method of photon beam production in this facility is given with discussions about the observed beam properties. The following part is organized by six sections, covering an overview of the beamline design (Sec. 2), laser injection and polarization measurement systems (Sec. 3), beamline equipment for the photon beam production and transportation (Sec. 4), the LEPS2 experimental build-

ing containing detector systems for hadron photoproduction experiments (Sec. 5), a detector system tagging high-energy photons generated by laser Compton scattering (Sec. 6), and the properties of a photon beam in the LEPS2 beamline (Sec. 7). Finally, a summary follows in Sec. 8 with future prospects.

## 2. Beamline design

For the photon beam production by laser Compton scattering, the LEPS2 beamline uses one of only four long straight sections in SPring-8. A length of the part without any magnets reaches 30 m in this straight section. In contrast, the LEPS beamline is constructed along one of the 40 usual straight sections, which are 7.8 m long. Electron beam divergence in the straight section influences the angular spread of a generated photon beam. The electron beam emittance of SPring-8 has become better from 2013 [25], and standard deviations ( $\sigma$ 's) of the electron beam divergence at the long straight section are currently 8 and  $0.7 \mu\text{rad}$  in the horizontal and vertical directions, respectively. This divergence is much better than that of the 7.8 m straight section, where the  $\sigma$ 's are 57 and  $1.4 \mu\text{rad}$  in the above two directions.

In the head-on collision of laser and electron beams, the correlation between the backscattering angle of photons  $\theta$  and the amplified energy  $E_\gamma$  is kinematically determined by the following equation:

$$E_\gamma = \frac{k(1 + \beta_e)}{(1 - \beta_e \cos \theta) + \frac{k(1 + \cos \theta)}{E_e}} \quad (2)$$

This equation tells that photons generated by laser Compton scattering are emitted in a conical shape with a scattering angle depending on the photon energy, as shown in Fig. 1(a). Kinematically, the scattering angle  $\theta$  becomes 0 degrees at the maximum energy corresponding to the Compton edge. Actual scattering angles are influenced by the electron beam divergence as indicated with the filled areas in Fig. 1(a). These areas show the  $1\sigma$  spreads of scattering angles after smearing the horizontal divergences of the electron beams in the LEPS2 and LEPS beamlines. In other words, they express the realistic production angles of photons that are scattered

in the horizontal plane including the electron beam axis. There is a large discrepancy between the angular spreads in the two beamlines due to different electron-beam divergences.

Figure 1(b) shows the RMS of scattering angles in the horizontal projection plane as a function of the lower bound (or the threshold value) of a selected photon-beam energy range. Contributions from the energy range exceeding the threshold are integrated with weights according to the photon beam energy distribution. A size of the photon beam in the selected energy range is given by multiplying a tangent of this RMS value by a distance. The RMS values were obtained by simulating photon scattering directions which form an energy-dependent cone and convolving them with the electron beam divergence of the LEPS2 or LEPS beamline. The evaluated horizontal angular spread for the LEPS2 beamline is not much different from the result using the simple kinematics of laser Compton scattering without any convolution. The horizontal divergence of a photon beam in the LEPS2 beamline is suppressed to about  $30 \mu\text{rad}$  for the tagged energy range above 1.3 GeV. In the case of the LEPS beamline, the horizontal angular spread is calculated to be  $62 \mu\text{rad}$  by the same procedure except for changing the lower bound of the tagged energy range to 1.5 GeV. The smaller angular spread in the LEPS2 beamline allows the transportation of a photon beam to a location far from the Compton scattering point, so that the LEPS2 experimental building containing large detector systems has been constructed about 130 m downstream. The photon beam size in the LEPS2 experimental building is suppressed to  $\sigma \sim 4 \text{ mm}$  for the tagged energy range. As suggested by Fig. 1(b), a size variation of the photon beam can also be observed depending on the photon energy region in the LEPS2 beamline, but not in the LEPS beamline.

The LEPS2 beamline is designed to make it possible to inject a maximum of four laser beams simultaneously. Each incident laser beam is expanded to a  $1/e^2$  diameter of about 40 mm by a beam expander to focus on a narrow spot corresponding to the electron beam size at the Compton scattering point, which is about 31.5 m away from the laser injection system. The four expanded laser beams are injected into the

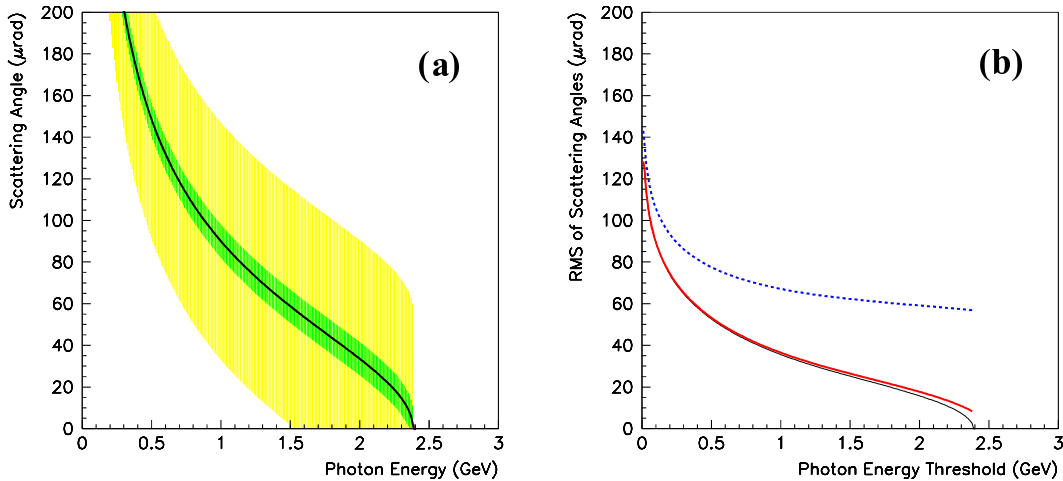


Figure 1: (a) The energy dependence of Compton scattering angles for photons produced in a conical shape (black line). The kinematics was calculated in the case of injecting laser light with a wavelength of 355 nm into SPring-8. The green and yellow areas indicate the  $1\sigma$  spreads when the horizontal divergences of the electron beams in the LEPS2 and LEPS beamlines are smeared, respectively. (b) The RMS of scattering angles in the horizontal projection plane for the photon-beam energy range exceeding the threshold shown in the x-axis. The conditions of photon beam production are the same as those for (a). The black thin solid, red thick solid, and blue dashed lines show the cases for the kinematics of laser Compton scattering, the LEPS2 beamline, and the LEPS beamline, respectively.

storage ring so that their profiles should be in contact with each other by arranging the central axes of four incident laser beams at the vertices of a square. Increase of the overall incident laser power causes a higher intensity of the photon beam, although the intensity gain is not fully proportional to the total power due to laser incident angles relative to the electron beam. An ideal gain factor of the photon beam intensity by the four laser injection has been simulated as shown in Fig. 9 of Ref. [1]. It is evaluated to be 2.14. Furthermore, we are improving the photon beam intensity also by introducing high-power lasers with a wavelength of 355 nm, which is currently chosen for normal operations. So far, such UV lasers with the output powers of 16 and 24 W have been installed in addition to 8 W lasers, which have been mainly used in the LEPS beamline.

The explained injection method using multiple lasers also enables the minimization of photon beam loss during its transportation from the Compton scattering point to the LEPS2 experimental building. The center of the square whose vertices correspond to

the four laser beam axes is a peripheral or low power-density part of any laser light. It is also a region that becomes the path of a photon beam produced by laser Compton scattering. Therefore, a hole has been made in the center of a mirror that reflects the four laser beams toward the Compton scattering point. This procedure has reduced the amount of beamline materials, maximizing the number of photons reaching the LEPS2 experimental building.

Propagation of the laser light follows Gaussian beam optics. When a designed value of the laser beam size is set at a focusing point (or the Compton scattering point), the magnification of a beam expander is uniquely determined as a function of the focal length. (See Eq. (2) of Ref. [1].) As this length becomes longer, it is necessary to increase the magnification factor and correspondingly enlarge the apertures of optical devices (e.g. reflection mirrors) and ultra-high vacuum chambers for laser beam paths. In order to make the focal length as short as possible in the LEPS2 beamline, laser beams are orthogonally injected into a beamline chamber through a hole at

a side concrete wall of the storage ring tunnel and reflected to the long straight section by a mirror in a vacuum.

Vacuum chambers connected to the long straight section have a special specification that cuts the internal diameter larger than the normal aperture for synchrotron radiation. Sufficient apertures that four laser beams go through are secured. A bottleneck of the laser beam passage exists in the vertical opening of a vacuum chamber inside the bending magnet that is 13.5 m away from the Compton scattering point. This vertical opening is enlarged to a maximum of  $\pm 20$  mm, accepting  $2.5\sigma$  regions of the laser beam profiles. The internal aperture of the LEPS2 beamline has a margin allowing even elliptical focusing of laser beams with a cylindrical expander [1] as a future option. In this case, by doubling the cross section of an incident laser beam only in the vertical direction, the vertical beam size at the focal point can be halved with twice the power density. Such laser beam shaping will enhance the efficiency of Compton scattering with the stored electron beam, whose cross section is flat having the horizontal and vertical sizes ( $\sigma$ ) of 340 and 10  $\mu\text{m}$ , respectively.

Figure 2 shows an outline drawing of the LEPS2 beamline. Laser oscillators and a part of optical devices are arranged on a surface plate in the laser injection room with an area of approximately 5 m  $\times$  8 m. As described above, multiple laser beams are merged so as to be adjacent to each other after the beam sizes are individually magnified by beam expanders. The merged beams are then guided into the storage ring tunnel by using three large mirrors with a diameter of 150 mm. As a laser beam path, a hole with a diameter of 160 mm is drilled through the 1-m thick concrete wall that forms the storage ring tunnel. A radiation protection hatch is constructed only around this hole in the experimental hall of the storage ring building. One of the three large mirrors mentioned above is placed in the radiation protection hatch.

The laser beams entering the tunnel are injected into a beamline chamber of the “front-end” section from its side entrance port. Chambers in the front-end section are directly connected to the storage ring on the extension of the long straight section with a

ultra-high vacuum, which is typically around  $10^{-8}$ – $10^{-7}$  Pa. Inside the chamber that has the side entrance port, the “first mirror” has been installed to reflect the incident laser beams to the upstream long straight section. In addition, the “monitor mirror” which drives up and down has been set up in a different chamber 0.7 m upstream of the first mirror. In the case of extracting the incident laser beams to the polarization measurement system, the laser beam direction can be changed to the outside of the front-end section by the monitor mirror. The monitor mirror is retracted upward when a photon beam is generated by laser Compton scattering.

The laser beams pass through the bending magnet, and then travel through the straight chambers that are also commonly used as the stored electron beam path. The section of those straight chambers is equipped with quadrupole and sextupole magnets for a distance of 10 m. Finally they reach the 30-m long straight section where no magnets exist. The beamline is designed to cause Compton scattering at a position about 2 m after the laser beams enter this straight section. At a location 8.4 m upstream from the Compton scattering point, there is a vacuum chamber that monitors laser spots and allows visual confirmation of the laser beam axes.

A photon beam generated by laser Compton scattering returns in the opposite direction of the incident laser-beam path. Recoil electrons which have lost energies due to Compton scattering also follow the same path. Their trajectories are largely bent to the inner side of the storage ring at the bending magnet. A detector for recoil electrons, called “tagger”, is installed downstream of the bending magnet to measure the hit position of a recoil electron whose trajectory differs depending on its momentum. A photon beam, which is a flux of high-energy  $\gamma$  rays, goes straight through the bending magnet and passes through a hole made at the center of the first mirror without loss due to electron-positron pair creation. After exiting a front-end vacuum chamber through a 2-mm thick aluminum window, it passes through a collimator and a sweep magnet. The collimator is located 24.5 m downstream from the Compton scattering point.

From downstream of the sweep magnet, the pho-

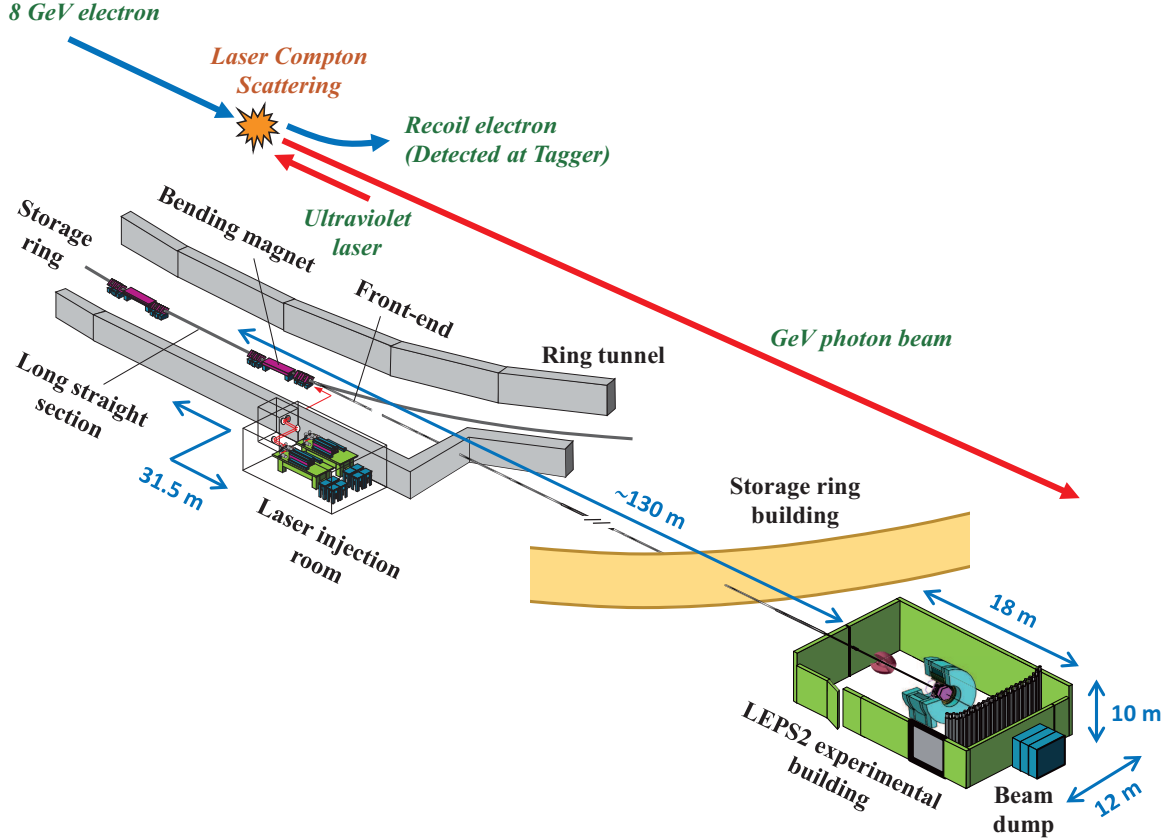


Figure 2: A conceptual overview of the LEPS2 beamline.

ton beam enters a transport pipe with a vacuum of about 10 Pa, and goes out of the storage ring tunnel. This transport pipe connects a long distance from the storage ring building to the LEPS2 experimental building, which is constructed about 130 m downstream from the Compton scattering point. The photon beam is extracted into the atmosphere from the transport pipe, and delivered to the detector systems that are set up for hadron photoproduction experiments in the LEPS2 experimental building. The height of the LEPS2 beamline is set to 1200 mm inside the storage ring tunnel, and 1400 mm in all other places.

### 3. Laser injection system

Figure 3 is a plan view of the section related to laser beam injection in the LEPS2 beamline. The optical system is built on a surface plate in an aluminum booth, called the laser injection room. This booth is made as a simple clean room under the condition of ISO class 7. We have operated UV lasers with a wavelength of 355 nm and an output power of 8, 16, or 24 W (Paladin Advanced, manufactured by Coherent Inc.[26]). Deep-UV lasers with a wavelength of 266 nm are also usable on another surface plate. As shown in Fig. 4, two stages are prepared with different heights, and four UV lasers are installed so that two of them should be placed on each stage. A

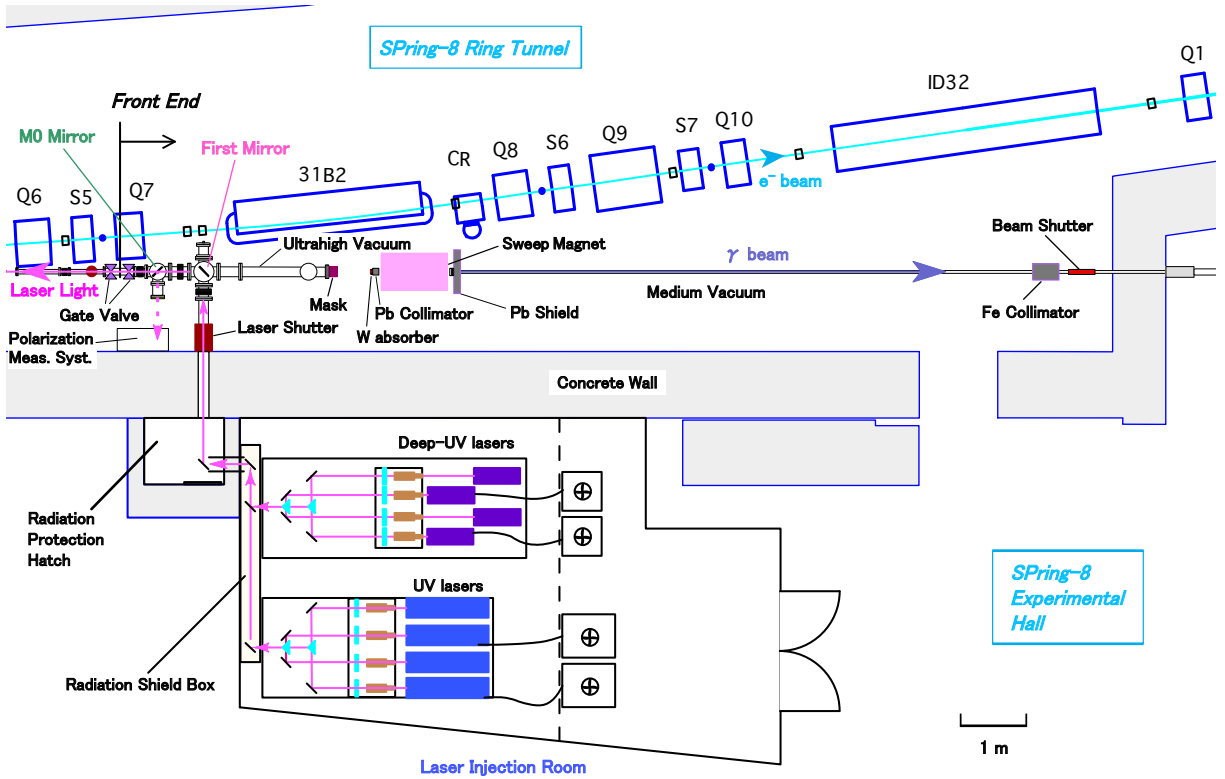


Figure 3: A plan view of the front-end section with the laser injection system in the LEPS2 beamline.

laser beam output from the individual oscillator is optically controlled by a set of a beam expander, a waveplate, and two mirrors.

The beam expander expands the  $1/e^2$  diameter of an incident UV laser beam from 1.35 mm to about 40 mm for the purpose to make a focus at the Compton scattering point, which is located 31.5 m ahead. On the basis of Gaussian beam optics [1, 2], the focal length is adjusted by changing a magnification factor of the beam expander, where a distance between the concave (input) and convex (output) lenses is optimized by a micrometer. This adjustment is finally accomplished by maximizing a Compton scattering rate or a photon beam intensity, measured by the tagger described in Sec. 6.

The two mirrors on the surface plate are used to adjust the direction and position of a laser beam injected into the storage ring. They are made of a syn-

thetic quartz substrate with a diameter of 80 mm. Their reflective surface is treated with a dielectric coating giving a reflectance of almost 100% at a wavelength of 355 nm. One of the two mirrors reflects laser light in the vertical direction, and the other in the horizontal direction at a proper height to make collisions with the electron beam. Each mirror is mounted on a dual-axis automatic precision stage that rotates in two orthogonal directions. A combination of the two mirrors enables the direction change and parallel shift of an incident laser beam. The automatic precision stage can be remotely controlled from the outside of the laser injection room, and the mirror angle can be adjusted in increments of approximately  $30 \mu\text{rad}$ .

A laser beam whose axis has been adjusted by the above two mirrors are further reflected in a direction parallel to the beamline at a reflective surface of a prism mirror. This mirror is made of a syn-

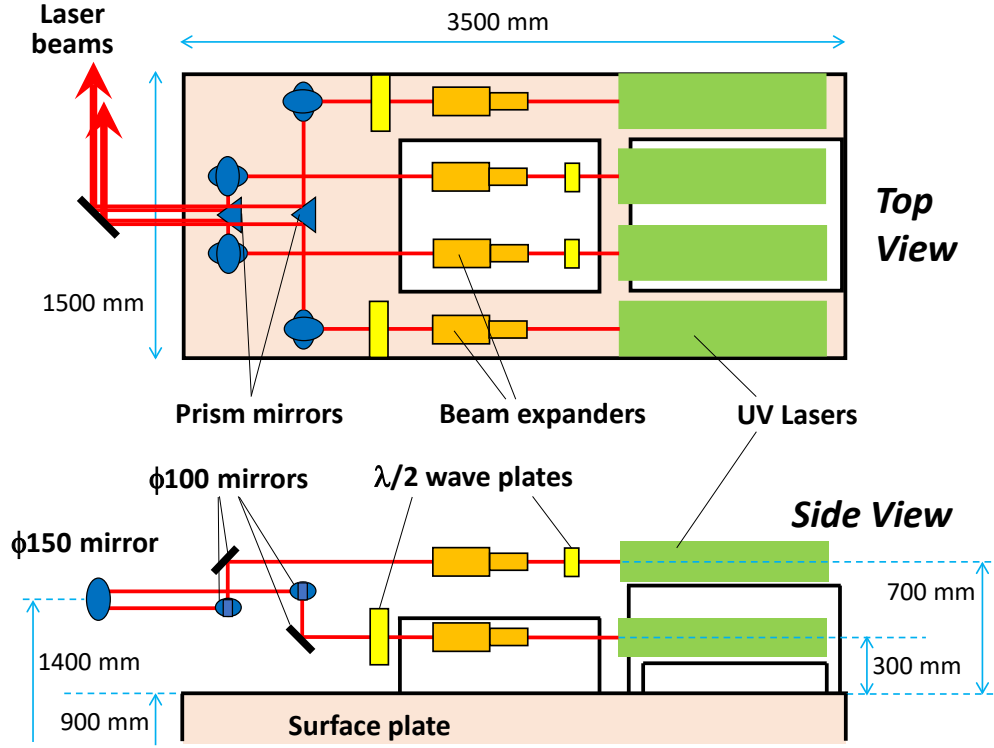


Figure 4: The optical system to simultaneously inject four laser beams into SPring-8. All devices are on a large surface plate.

thetic quartz right-angle prism with two orthogonal reflective surfaces, each of which has a size of  $80 \text{ mm} \times 80 \text{ mm}$ . The reflective surface is coated exclusively for a wavelength of  $355 \text{ nm}$ . Two different laser beams at the same height are individually redirected by the two reflective surfaces, and merged into adjacent beams traveling in the same direction. There are two prism mirrors with slightly different heights to handle four laser injection by making two sets of side-by-side beams vertically adjacent. The four laser beams are simultaneously guided into the storage ring tunnel by using three large mirrors with a diameter of  $150 \text{ mm}$ . These large mirrors are made by applying a dual-wavelength coating for  $355$  and  $266 \text{ nm}$  on a circular substrate of synthetic quartz. The two prism mirrors and the three large mirrors are individually mounted on manual precision stages. The setting of their positions, heights, and angles was fixed after the adjustment in the initial stage of beamline operation.

Inside the laser injection room, two of the three large mirrors and the merged laser-beam paths between them are shielded by a lead-plate box with a thickness of  $3 \text{ mm}$ . Thanks to this radiation shield, we can perform manual adjustment and maintenance works for lasers and optical devices in the laser injection room even during the photon beam production. The other large mirror is set in an interlocked radiation protection hatch, which is located outside the laser injection room and covers a  $160\text{-mm}$  diameter hole for laser beams entering the storage ring tunnel. This hatch is constructed by concrete walls in a small area of  $1.5 \text{ m} \times 1.7 \text{ m}$ . For the hole drilled through a side wall of the storage ring tunnel, we put a motor-driven laser shutter made of iron with a thickness of  $400 \text{ mm}$ . It can be remotely closed inside the tunnel for radiation shielding when laser beams are not injected.

In the storage ring tunnel, the incident laser light

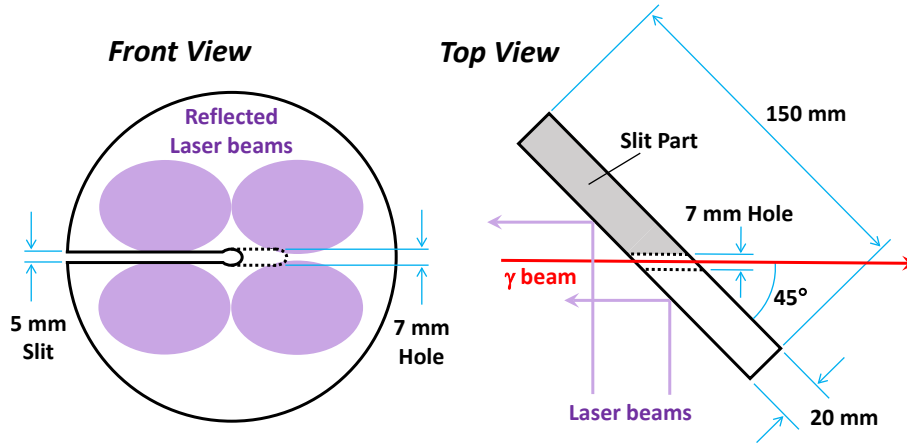


Figure 5: Front and top views of the first mirror installed in a front-end vacuum chamber. Four laser cross sections reflected at this mirror are also indicated by smaller purple circles.

enters a front-end chamber from a side viewport with a ConFlat flange size of ICF203 (DN160). This viewport has a synthetic quartz window with an effective diameter of 140 mm and a thickness of 8 mm. Its transmittance for UV wavelength light is about 94%. The incident laser light is then reflected toward the long straight section by the first mirror tilted 45 degrees with respect to the beamline direction. The first mirror is made of an aluminum-coated silicon substrate with a diameter of 150 mm and a thickness of 20 mm. Its reflectance is about 90% in a UV wavelength region. As shown in Fig. 5, a 5-mm wide slit is horizontally machined at the electron beam height in the half area closer to the storage ring. This structure allows synchrotron radiation of X rays to escape without heat load to the first mirror, whose reflective surface can be distorted by non-uniform temperature rise. Moreover, a water-cooled oxygen-free copper plate is applied to the back surface of the mirror in order to remove heat that is generated by a halo component of the synchrotron radiation hitting the edges of the slit. An entire mirror holder with the cooling plate is fixed by three columns that can be manually moved back and forth. The position and angle of the first mirror have been adjusted at the beginning of LEPS2 beamline operation by using these columns.

At the first mirror, four incident laser beams are

reflected in a square positional relationship as shown in Fig. 5. The reflected laser beams are focused at the Compton scattering point 22 m ahead from the first mirror, and collide with the stored electron beam. A high-energy photon beam generated by Compton scattering travels back to the first mirror, and passes through its central hole with a diameter of 7 mm. This hole is made along the photon beam path from the center of the reflective surface with a tilting angle of 45 degrees. This structure is important to eliminate the photon beam loss due to electron-positron pair creation.

The laser light is almost 100% linearly polarized when it is emitted from an oscillator. The direction of linear polarization is controlled by using an optical element called a  $\lambda/2$  waveplate, which causes a phase difference of half a wavelength between two orthogonal polarization components. Because the LEPS2 facility uses high-power lasers, we have adopted a zero-order quartz waveplate with an air gap. In the laser injection room, a  $\lambda/2$  waveplate is installed at the exit of each laser oscillator, and is rotated around the laser beam axis to adjust the direction of linear polarization horizontally or vertically. This rotational adjustment is done in the same way for all the laser beams that are simultaneously injected. The polarization direction is alternately changed about every

week during the collection of physics data. The laser light immediately after the emission from an oscillator has a high power density, so that an irradiation position on the  $\lambda/2$  waveplate is periodically shifted to avoid significant damage. For reducing such damage, a large  $\lambda/2$  waveplate with a diameter of 60 mm has been also introduced to control the polarization after magnifying a laser beam diameter by a beam expander. But the production cost of large waveplates is high and the installation of them is limited for a part of multiple laser beams. In the case of making circular polarization, an optical element called a  $\lambda/4$  waveplate will be placed downstream of the  $\lambda/2$  waveplate.

The polarization of a photon beam produced by Compton scattering is calculated by inputting that of laser light into Eqs. (16) and (17) of Ref. [17] for linear and circular polarization states, respectively. The linear polarization is highest at the Compton edge, and gets lower as the photon beam energy decreases. The polarization of laser light acts as a scale factor for that of a photon beam in the above calculation. Here it is important to measure the linear polarization of laser beams just before Compton scattering because it may be deteriorated by reflections at many mirrors. This deterioration can happen by slightly different reflectances for the S- and P-wave components of laser light, which are defined by the direction of linear polarization with respect to the plane of incidence [16]. Therefore, the polarization measurement is regularly performed by inserting the monitor mirror on a laser beam path, as mentioned in Sec. 2, and extracting the laser light from a synthetic quartz viewport of a front-end vacuum chamber in the direction to the outer periphery of the storage ring.

The extracted laser light is incident on the polarization measurement system contained by a lead radiation shielding box in the storage ring tunnel. A main unit of the polarization measurement system consists of a polarizer (Glan Laser prism made of calcite) that rotates by remote control and a silicon photodiode (S8746-01 manufactured by Hamamatsu Photonics K.K.) that measures an intensity of the laser light after passing through the polarizer. A neutral-density filter for dimming is inserted between

the polarizer and the photodiode. For linearly polarized laser light, the above unit measures a sine curve of the transmitted light intensity, where the maximum and minimum values ( $P_{\max}$  and  $P_{\min}$ , respectively) appear alternately depending on the rotation angle of the polarizer. The linear polarization is given by the calculation of  $(P_{\max} - P_{\min}) / (P_{\max} + P_{\min})$ . In the operation so far, the measured polarization was typically about 98% and there was no significant difference between the horizontal and vertical polarization states. Because four laser beams that are simultaneously injected reach different positions in the polarization measurement system, the unit of the polarizer and the photodiode is mounted on a stage that moves to the position of each laser beam by remote control.

#### 4. Beamline chambers and transport line

Figure 6 shows a plan view of the LEPS2 beamline from the downstream part of the long straight section to the vicinity of the tagger, which is located downstream of the bending magnet. The explanation of newly produced and modified chambers for the construction of the LEPS2 beamline can also be found in Ref. [27]. Laser Compton scattering is designed to occur at a place that the laser light reaches after entering the 30-m long straight section and traveling a distance of 2 m. Most of the unscattered laser light goes upstream of the storage ring, but cannot escape from the viewport on the opposite side of the straight section, being repeatedly reflected by the inner walls of vacuum chambers. Such laser reflections inside the storage ring can cause vacuum deterioration that is not negligible in maintaining an ultra-high vacuum. Therefore, beamline baking with laser injection is regularly performed during the shutdown periods of the storage ring.

In order to know the directions of incident laser beams, it is necessary to install a dedicated chamber where laser beam spots can be observed before the inner reflections happen in the long straight section. This observation system is called the laser monitor. The 725-mm long chamber that was originally located 8.4 m upstream of the Compton scattering point is replaced with the laser monitor chamber

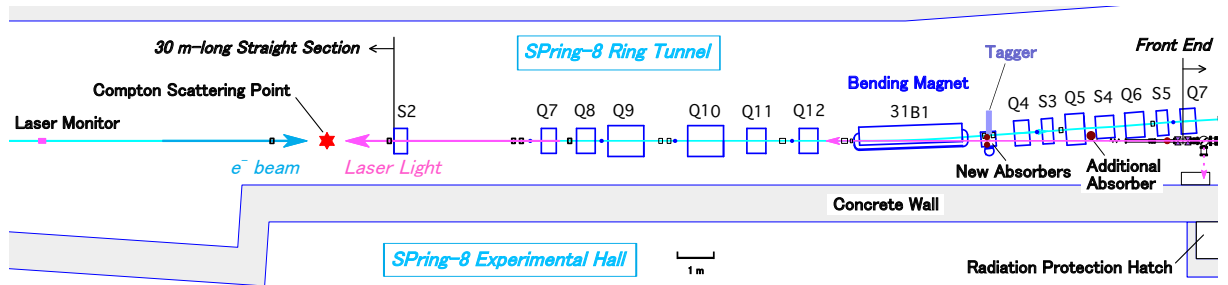


Figure 6: The upstream part of the LEPS2 beamline from the laser monitor to the bending magnet, where the accumulated electron orbit and the produced photon beam path are separated.

shown in Fig. 7. Inside this chamber, comb-shaped windows with many 1-mm wide slits are attached at an angle of 9 degrees on the upper and lower sides not to interfere with the surface current that accompanies the stored electron beam. A distance to the electron beam orbit is 8 mm at the closest points of the window structures. The laser light that has passed through either of the upper or lower slits hits an internal screen made of an alumina fluorescent plate, allowing the irradiated position to be observed from a CCD camera set in the atmosphere outside a viewport.

A high-energy photon beam produced by laser Compton scattering goes back on the path of the incident laser light in the opposite direction. After leaving the 30-m long straight section, the photon beam passes through straight chambers with quadrupole, sextupole, steering magnets, etc. for a distance of 10 m. Then, the photon beam path is separated from the accumulated electron orbit in a vacuum chamber set inside a gap of the bending magnet. In this chamber, the aperture for the photon beam path is widened as much as possible, as described in Sec. 2.

Highly brilliant synchrotron radiation of  $X$  rays is not only an unnecessary contamination for the GeV  $\gamma$ -ray beam but also a source of heat generation and vacuum deterioration due to their scattering at vacuum chambers and optical devices. Thus, two new  $X$ -ray absorbers are installed in the chamber just downstream of the bending magnet. They are attached instead of a conventional crotch absorber, and cover side areas of the photon beam path so as not

to interfere with the laser injection; One is placed on the accumulated electron orbit side to receive brilliant synchrotron radiation, while the other is put on the outer circumference side to absorb a halo component of  $X$  rays. For the chamber to which the new absorbers are mounted, further modification has been made on the inner side of the accumulated electron orbit; The chamber size is horizontally enlarged to secure the widespread path of recoil electrons, which lose energy by Compton scattering and are largely bent at the bending magnet. A horizontal-slit window made of 3-mm thick aluminum-alloy is attached to the modified chamber as the exit of recoil electrons. Recoil electrons extracted into the atmosphere are analyzed by the tagger to measure their momenta, as explained in Sec. 6.

After passing through the bending magnet, the photon beam further travels inside large-aperture straight chambers located in a 4-m long area beside a series of convergent magnets. Here, an additional  $X$ -ray absorber is installed to stop the horizontally spreading synchrotron radiation. This absorber is shaped in a narrow fin extended from the accumulated electron orbit side at the photon beam height. It is designed to avoid obstructing the laser injection but block a part of synchrotron radiation.

The photon beam then enters the section of front-end chambers which have the optical devices related to the laser injection. At an upstream chamber of the front-end section, the monitor mirror made of a 20-mm thick silicon substrate can be inserted downward, as mentioned in the previous sections. The mirror

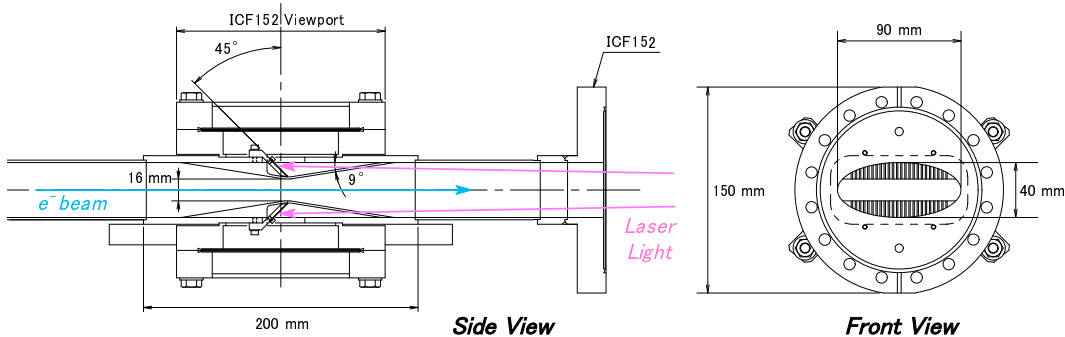


Figure 7: The laser monitor chamber installed 8.4 m upstream of the Compton scattering point in the straight section of the LEPS2 beamline. The ConFlat flange ICF152 (DN100) has an outer diameter of 152 mm.

substrate is horizontally tilted by 45 degrees to the beamline. It also serves as an absorber to prevent synchrotron radiation from penetrating downstream of the beamline when a photon beam is not generated. This mirror absorber can be remotely raised or lowered by compressed air operation when necessary.

The front-end vacuum section ends 2 m downstream of the first mirror or 24.1 m downstream of the Compton scattering point. The photon beam is once taken out into the atmosphere from a water-cooled ICF152 (DN100) flange with an aluminum window that is made thin down to 2 mm in a 10-mm diameter region. On the vacuum side of this window, an oxygen-free copper mask is attached with a water-cooling pipe. This mask receives synchrotron radiation in a rectangular part that has vertical and horizontal widths of 10 and 120 mm, respectively, with depth-direction slopes toward a narrow central area. The central area corresponds to a photon beam path with the thin aluminum window. A vacuum in the front-end section is maintained in the range around  $10^{-8}$ – $10^{-7}$  Pa by two ion and two titanium getter pumps.

The photon beam extracted into the atmosphere immediately passes through an  $X$ -ray absorber made of a 1-mm thick tungsten plate and a 7-mm diameter lead collimator with a length of 100 mm. In the LEPS2 beamline, the straight section common to the storage ring is much longer than that of the usual beamlines, so that there is a non-negligible amount of the contamination due to bremsstrahlung  $\gamma$  rays

generated by accumulated electrons passing through a residual gas inside the ring. Therefore, a broad angular component of  $\gamma$  rays are cut off by the collimator. Lower-energy  $\gamma$  rays have angular broadening in the kinematics of laser Compton scattering, so a component of the photon beam below about 0.5 GeV cannot go through the lead collimator, as recognized from Fig. 1.

A sweep magnet, which is a 1-m long neodymium magnet with a magnetic field of 0.63 T, is installed downstream of the lead collimator to remove the contamination of electrons and positrons produced by pair creation at the upstream materials. At a location 10 m downstream of the lead collimator, an iron collimator with a diameter of 11 mm and a length of 200 mm is placed to serve as a buffer collimator to shield secondary particles produced with large angles at the tungsten absorber and the aperture edge of the lead collimator. Downstream of the iron collimator, we put a beam shutter to provide radiation shielding when a photon beam is not generated. All the devices described above are located inside the 1-m thick concrete walls of the storage ring tunnel so as to avoid possible problems on radiation protection.

A photon-beam transport pipe with a medium vacuum of 10 Pa starts immediately downstream of the sweep magnet, and runs 95.6 m through the concrete wall of the ring tunnel and the experimental hall in the storage ring building. It extends to the LEPS2 experimental building, which is independently constructed for hadron photoproduction ex-

periments. The inner diameter of the transport pipe is 60 mm in the storage ring tunnel and gradually increases to 200 mm as it approaches the LEPS2 experimental building. On both ends of the transport pipe, thin films are attached as a partition between the atmosphere and a vacuum. A Kapton film with a thickness of 75  $\mu\text{m}$  (125  $\mu\text{m}$ ) and an aramid film with a thickness of 50  $\mu\text{m}$  (50  $\mu\text{m}$ ) are superimposed for the upstream (downstream) end. For putting the films safely on the downstream end of the transport pipe, its inner diameter is converted from 200 mm to 100 mm by adding a short straight pipe.

## 5. Experimental building

The LEPS2 experimental building is located at the most downstream of the LEPS2 beamline and has enough space to contain large detector systems covering most of all solid angles. The size of the LEPS2 experimental building is 18 m in the direction of a photon beam, 12 m in width, and 10 m in height. It is equipped with an overhead traveling crane allowing a maximum load of 2.8 t. Figure 8 shows a floor plan of the LEPS2 experimental building. In the future, this building can be expanded downstream to an area about 1.5 times larger. The downstream end of the photon-beam transport pipe is located at the most upstream part of the LEPS2 experimental building. A 200-mm thick lead shield with a 45-mm diameter hole is installed just downstream of the pipe end. This hole is slightly wider than the maximum spread expected for the photon beam that is cut off by the 7-mm diameter collimator in the storage ring tunnel. It prevents a halo component of the photon beam from entering the downstream detector systems. Further downstream but just upstream of the individual detector systems, additional lead shields or collimators are placed depending on the experiments. Charged particles contaminating the photon beam or generated by the halo component of the beam are rejected in the offline analysis by using a large plastic scintillator, called the UpVeto counter.

A beam dump, which receives all photons, is located at the downstream end of the LEPS2 experimental building [28]. A core of the beam dump is made of iron with a cross section of 400 mm  $\times$

400 mm and a depth of 300 mm. In front of the core, a 150-mm thick iron block having a 100-mm square hole along the photon beam axis is attached to absorb the backscatter of electromagnetic showers. The back and sides of those iron blocks are covered with 100-mm and 50-mm thick lead, respectively. The surrounding volume with a horizontal width of 2200 mm, a height of 2600 mm, and a beam-direction depth of 1800 mm is further filled with concrete. This structure allows a photon-beam intensity (a Compton scattering rate over all the energy range) up to  $5 \times 10^7 \text{ s}^{-1}$  in terms of the radiation safety. In addition, the outside area of the front part of the beam dump is reinforced with a 300–400-mm thick concrete shield wall to stop particles photoproduced with angular spread from the fixed target inside a detector system. The additional concrete wall is designed to permit a target thickness to be increased up to 0.1 radiation length in the LEPS2 experimental building. Almost all of the LEPS2 experimental building is set to a radiation controlled area, except for the front room with a size of 2.4 m  $\times$  7.5 m near the entrance. The amount of radiation leakage is reduced by taking a large space whose boundary is far enough from the fixed target and restricting access to this area with an interlock system.

Different detector systems are separately set up in the upstream and middle parts of the LEPS2 experimental building, and operated in different periods of the beamtime depending on experimental programs. Details of the individual detector systems will be described in separate articles. In the upstream area, a large-acceptance electromagnetic calorimeter “BGOegg”, which covers polar angles from 24 to 144 degrees, is installed with a fixed target at a distance of 125 m from the Compton scattering point. This calorimeter consists of 1,320 BGO crystals assembled in an egg shape, and a total length of the detector reaches about 1 m between the upstream and downstream ends. It excels in detecting photoproduced neutral mesons, decaying into multiple  $\gamma$  rays. The energy resolution for 1-GeV  $\gamma$  rays is 1.3% [29], corresponding to the highest performance in the world. The BGOegg is combined with charged-particle detectors that are installed onto its inner and forward sides to detect and identify all the final states of a

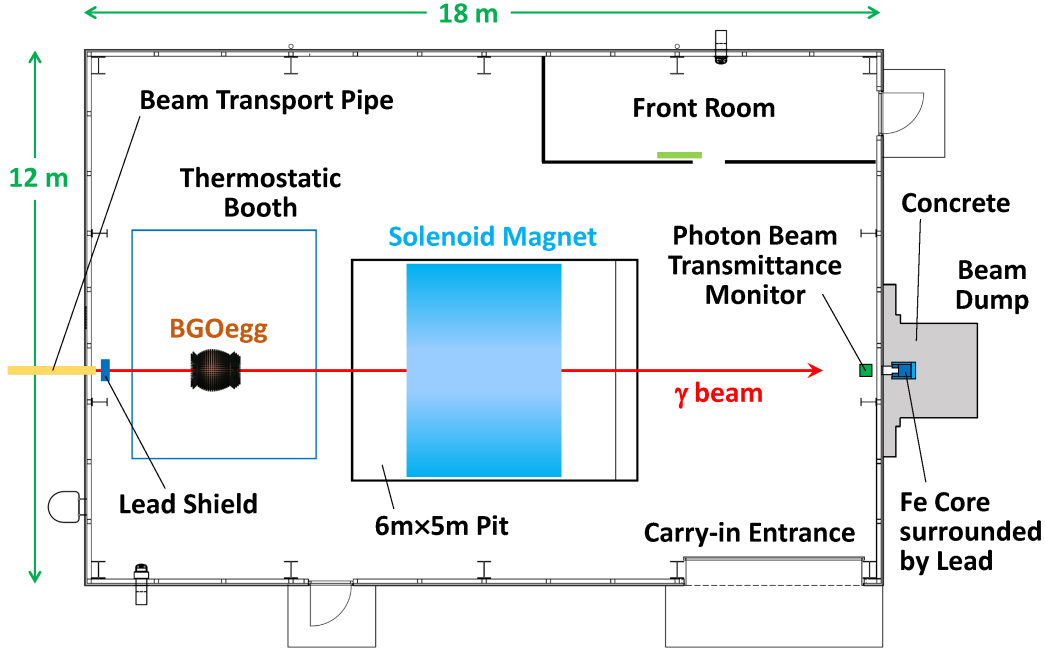


Figure 8: A plan view of the LEPS2 experimental building, located in the downstream end of the LEPS2 beamline.

hadron photoproduction reaction as much as possible. Because of temperature dependence in the amount of scintillation light of a BGO crystal and the signal output of a photomultiplier tube, the entire detector system is housed in a thermostatic booth with an area of  $5.2 \text{ m} \times 4.2 \text{ m}$ . The detector system with the BGOegg calorimeter is already under operation. Physics data-taking using a liquid hydrogen or carbon target was done from 2014 to 2016. So far, we have shown results in the analyses searching for baryon resonances and mesic nuclei [30, 31, 32].

In the center of the LEPS2 experimental building, there is a pit with an area of  $5 \text{ m} \times 6 \text{ m}$  and a depth of 1.5 m. The center of the pit is 131 m away from the Compton scattering point. A large solenoid magnet weighing 400 t with a diameter of 5 m and a length of 3.5 m has been relocated to this pit from the E787/E949 experiment [33] at Brookhaven National Laboratory. The central axis of the solenoid magnet is aligned along the photon beam. Inside the

2.96-m diameter bore with a central magnetic field of 1 T, we have set up a large charged-particle spectrometer, which consists of a time projection chamber, four planar drift chambers, and many types of particle identification detectors [34]. Data acquisition using a liquid hydrogen or deuterium target is beginning for studying the photoproduction of a pentaquark  $\Theta^+$ , which is attracting attention as an exotic hadron [35, 36], and a hyperon  $\Lambda(1405)$ , which is expected to have a hadronic molecular structure [37, 38]. The use of a large solenoid magnet with normal conductivity scales up the infrastructure of the LEPS2 experimental building by requiring a unit receiving and transforming an electric power up to 2 MVA and a cooling water system with a capacity of 1.5 MW as ancillary equipment.

## 6. Photon tagger

The tagger detects recoil electrons whose energy is lost by laser Compton scattering. As shown in Fig. 6, it is installed near the exit of the 0.68-T bending magnet downstream of the long straight section. It is located on the inner circumference side of the storage ring to measure the momentum of a recoil electron. From the four-momentum conservation in laser Compton scattering, the measured electron momentum is converted to the energy of a backscattered photon event by event. In addition, the integrated number of scattered photons during an experiment is obtained by counting the number of recoil electrons detected at the tagger, and used to measure the cross sections of hadron photoproduction reactions. The detection of a recoil electron also serves to generate a trigger signal for physics data acquisition.

The detector structure of the tagger is shown in Fig. 9. Two layers of bundles made of 1-mm square scintillating fibers are arranged in the upstream side, while two layers of plastic scintillators having a width of 8 mm, a thickness of 4 mm, and a height of 10 mm are placed in the downstream side. Six scintillating fibers are bundled into a single readout channel by lining them up in the direction of a recoil electron track to increase a detection efficiency. The recoil electron whose trajectory has been bent at the bending magnet changes a hit position in the tagger depending on its momentum. The digitization of hit positions is subdivided by installing the two fiber-layers with a 0.5 mm shift to each other. Correspondingly, the measurement of a photon beam energy is digitized by about every 15 MeV, resulting in the detector resolution of  $15/\sqrt{12} = 4.3$  MeV.

The plastic scintillators in the downstream side are arranged so that two channels in different layers should be paired with geometrical overlap in the direction of a recoil electron path. A pair of plastic scintillators covers an about 240 MeV range of the photon beam energy. The 2-mm wide region at the edge of each scintillator overlaps with that of an adjacent scintillator. The overlapped region corresponds to a photon beam energy range of about 60 MeV. If a recoil electron passes through this region, four plastic scintillators have hit signals.

The position of individual scintillating fiber bundles and plastic scintillators in the same layer is shifted downstream as they are away from the electron beam orbit toward the inner side. This arrangement is adopted because a large amount of  $X$  rays by synchrotron radiation are scattered at an absorber in the vacuum chamber immediately downstream of the bending magnet. The entire tagger is enclosed in a shield box to prevent these  $X$  rays from entering the signal-sensitive parts. The layers of scintillating fibers and plastic scintillators are arranged in a shadow of the shield-box wall on the storage ring side. The shield box is made of 1-mm thick copper and 2-mm thick lead plates. A part of the shielding wall where  $X$  rays are particularly intense on the storage ring side is made of a 3-mm thick tungsten plate instead of the lead plate. Only in the area that recoil electrons go through, a narrow window is left on the upstream wall of the shield box.

A 16-channel multi-anode photomultiplier tube (H6568-200MOD by Hamamatsu Photonics K.K.) and a metal-package photomultiplier tube (R9880U-210 by the same manufacturer) are used to read signals from scintillating fiber bundles and a plastic scintillator, respectively. For the readout of a scintillating fiber signal, only the detection time of a recoil electron is recorded in data collection, and the gain of a photomultiplier tube is adjusted before the data-taking by determining the applied voltage to an optimum value giving an enough detection efficiency. On the other hand, both the detection time and energy are recorded as data for a plastic scintillator signal.

A recoil electron track is reconstructed under the conditions that one or two layers of scintillating fibers and both layers of plastic scintillators have coincident hits and that the positions of hit fibers and scintillators are geometrically on a straight line nearly parallel to the accumulated electron orbit. The hit timing of a plastic scintillator is tightly required to be consistent with that of a paired plastic scintillator in the other layer. The detection time of a recoil electron track is calculated by averaging the hit timings of plastic scintillators. When multiple recoil-electron tracks are found in one recorded event, only one track that is associated with a physics reaction can be selected by requiring its detection time to be

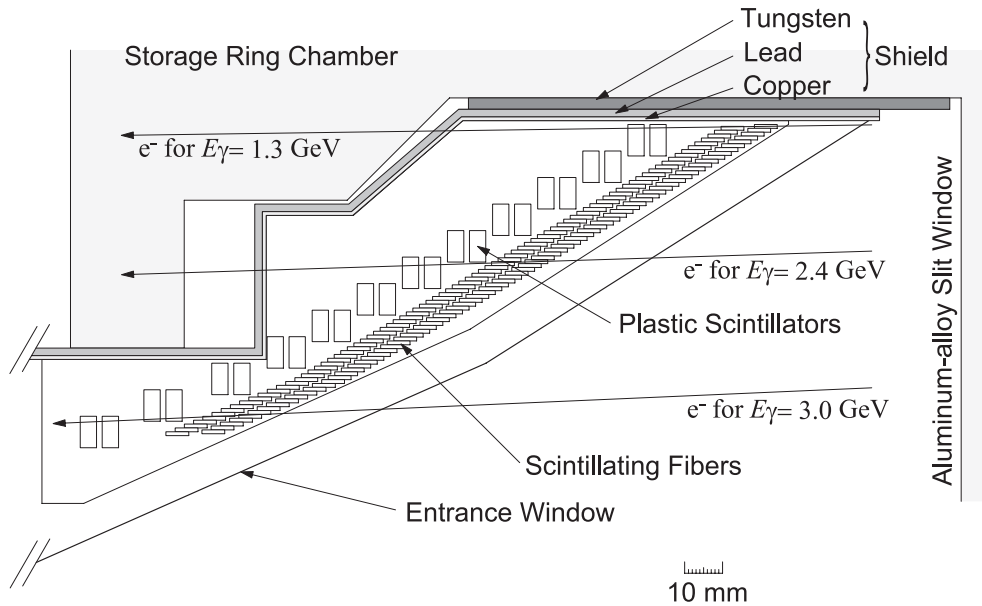


Figure 9: A plan view of the tagger with two layers of scintillating fibers (upstream) and two layers of plastic scintillators (downstream).

consistent with the reaction timing determined by a detector system in the LEPS2 experimental building. However, the track selection is impossible if multiple recoil-electron tracks are detected without a time difference larger than 2 ns, which corresponds to the minimum bunch interval of the stored electron beam. In this case, a true photon beam energy cannot be identified for a hadron photoproduction event. Such an event was discarded in physics analyses.

Recoil electrons that have not lost large energy at Compton scattering pass near the accumulated electron orbit without entering the tagger. Therefore, there is a lower limit to the photon beam energy that can be measured. It is 1.26 GeV for the case of the LEPS2 beamline. Calibration of the photon-beam energy determination at the tagger was performed by comparing the hit position of a recoil electron with a photon energy predicted in an independent measurement. Here, the detector system in the LEPS2 experimental building can measure all the final-state particles of a hadron photoproduction event, and it is possible to evaluate a photon beam energy from the kinematic fit that does not use the tagger infor-

mation. In this energy calibration, a quartic function was fitted to the correlation between the predicted energy and the hit fiber position. This fit was constrained by an additional condition that the polynomial function should represent the maximum photon beam energy, calculated based on Eq. 1, at the Compton edge observed in the distribution of hit fiber positions.

The reconstruction efficiency for a recoil electron track is mainly determined by the following three sources: (i) a percentage of a straight track that is successfully reconstructed from a combination of scintillating fibers and plastic scintillators, (ii) a rate to find only one track that can be separated at a reaction time for a certain event, and (iii) detection efficiencies of the scintillating fibers for which discriminator thresholds become effectively high when the gains of photomultiplier tubes drop. This efficiency is evaluated by using a data sample in which the photon beam energy can be obtained independently of the tagger information, as done in the energy calibration. The efficiency value varies depending on the hit position of a tagger track or the photon beam en-

ergy because of the source (iii). Its typical value is estimated to be around 90%.

A tagger trigger signal, which is a logic signal with a width of 20 ns, is generated when there is at least one pair of coincident hits at geometrically overlapped channels in the two layers of plastic scintillators. This signal is incorporated as a part of the hadron photoproduction trigger required for physics data acquisition. It is also used to measure the intensity of a tagged photon beam by counting the number of signals at a scaler. The integrated number of tagger trigger signals is important for calculating the luminosity of collected data. In the measurement of a photon beam intensity, it is not possible to separate time difference equal to or less than the width of the tagger trigger signal, so it is necessary to correct dead time. This correction is purely stochastic, and influenced by the filling pattern of electron beam bunches at SPring-8 [39]. The amount of dead time correction increases as a length of bunch trains, where electron bunches are filled every 2 ns according to the radio frequency applied to the accelerator, becomes longer. In contrast, the amount of correction is smaller when electron bunches are filled at equal intervals every several tens of ns. Moreover, a larger dead time correction is needed as the photon beam intensity itself increases. Such correction factors are obtained by a Monte Carlo simulation depending on the filling pattern and the beam intensity.

The tagger trigger counts are affected by the contamination originating from high-momentum recoil electrons, which take the paths closer to the accumulated electron orbit and thus should not be tagged in principle. A part of these recoil electrons hit a side wall of the tagger shield box or a vacuum chamber structure to extract recoil electrons into the tagger. The electron hit can cause an electromagnetic shower that leaves signals at the sensitive parts of the tagger. A contamination rate of the shower contribution in the tagger trigger counts is estimated to be 4.2% for the LEPS2 beamline. This rate is much lower than that of the LEPS beamline ( $\sim 21\%$ ) because we have cut off a wall structure separating the storage ring and the space expanded for recoil electron paths inside the vacuum chamber just upstream of the tagger. In the offline reconstruction of a recoil

electron track, the contamination of an electromagnetic shower is removed by tightening the conditions of geometrical correspondence among hits in multiple layers and limiting the number of hit fibers that can be continuously connected as a cluster in a certain layer.

## 7. Photon beam properties

The construction of the LEPS2 beamline started in 2010, and the first observation of photon beam production was successfully done in January 2013 [23]. After commissioning, the first phase of full-scale data collection was carried out from 2014 in the experiments using the BGOegg calorimeter. In the operation so far, only UV lasers with a wavelength of 355 nm have been used. Depending on experimental periods, two to four laser beams were simultaneously injected into the storage ring. The number of lasers in use often decreases from the maximum of four because some of oscillators alternately need to be overhauled for about half a year due to the deterioration of inner optics by aging. We currently operate one and two high-power lasers with outputs of 24 W and 16 W, respectively, and additionally use old oscillators with an output power of 8 W at remaining slots for multiple laser injection. The optical system for laser injection is damaged due to the long-term irradiation of laser light and the leakage of X rays by synchrotron radiation. Since the transmittance and reflectance of optical devices decrease, they should be renewed as appropriate. In particular, the first mirror and synthetic quartz window installed in a front-end vacuum chamber need to be replaced once every few years. For deep-UV lasers, we will proceed with their installation in the future after the development of high-power oscillators has been achieved, as described in Sec. 8.

The intensity of a photon beam reaching a target for hadron photoproduction experiments in the LEPS2 experimental building is estimated by correcting the counting rate of tagger trigger signals with the simulated dead time and the shower contamination rate, explained in Sec. 6. Then, the corrected tagger rate must be multiplied by the beamline transmittance for photons traveling a distance of about 130 m.

A time-integrated value of the photon beam intensity is important for obtaining the differential cross sections of hadron photoproduction reactions measured in the detector system around the target. As already mentioned, there are various materials on the photon beam path from the Compton scattering point to the fixed target in the LEPS2 experimental building, causing conversions to electron-positron pairs. Here, the beamline materials refer to the aluminum window at the exit of the front-end section, the tungsten X-ray absorber, the Kapton and aramid films attached to both ends of the photon-beam transport pipe with a medium vacuum, the air space after leaving the front-end section or the beam transport pipe, and the UpVeto counter. The transmittance calculated from the amount of these materials is 77.2%, where the influence of the 1-mm thick tungsten plate is the most effective. On the other hand, the LEPS beamline has a structure in which a photon beam passes through a silicon mirror in a vacuum [1], providing a lower transmittance of about 67%.

Recently, a system to measure the photon beam transmittance by counting a rate of pair creation with a converter has been developed to be installed upstream of the beam dump in the LEPS2 experimental building [40]. The ratio of counting rates in this system and the tagger will be immediately monitored during experimental periods. The measured transmittance is in agreement with the value calculated from the amount of materials. So far, we have observed a phenomenon in which the transmittance depends on the photon beam energy when the focal point of incident laser light shifts farther than the design, causing the cut-off of a lower-energy and more-widespread component of the photon beam at the lead collimator [30, 40]. Therefore, it is important to monitor the laser focal point through the confirmation of no existence of energy dependence in the transmittance measured with this system.

In the LEPS2 beamline, the maximum rate of tagged photons, obtained based on the tagger trigger rate with the corrections for dead time and shower contamination, has reached  $3.0 \times 10^6 \text{ s}^{-1}$  by injecting the UV laser beams into the storage ring with an electron beam current of 100 mA. After multiplied by the beamline transmittance, this rate corre-

sponds to a photon beam intensity of  $2.3 \times 10^6 \text{ s}^{-1}$  in the LEPS2 experimental building. The photon beam intensity at an experimental setup has increased by approximately 25% compared with the case that two UV laser beams are injected in the LEPS beamline. At the moment, the tagger trigger rate in the LEPS2 beamline is not as high as initially expected. This problem arises from the difficulty to precisely adjust the optimum axes of incident laser beams due to the deterioration of a vacuum during the storage ring operation. The vacuum deterioration occurs by repeated reflections of the laser beams inside the storage ring chambers, so that the beamline baking must be performed by laser injection with fixed beam axes before the ring operation, as explained in Sec. 4. We plan further improvement of the tagger trigger rate to be realized after the introduction of pulsed lasers, described in Sec. 8.

When laser beams are not injected,  $\gamma$  rays by bremsstrahlung from the residual gas in the electron storage ring are generated in the form of a beam. In the LEPS2 beamline, a portion that is common with the storage ring is as long as 50 m, including the 30-m long straight section without any magnets and the additional 10-m long parts at both ends with convergent magnets. So the tagger trigger rate by bremsstrahlung  $\gamma$  rays becomes  $(1-2) \times 10^4 \text{ s}^{-1}$ , which is an order of magnitude more than that in the LEPS beamline with a straight section of 7.8 m. When laser beams are injected, the bremsstrahlung  $\gamma$  rays are mixed in a tiny fraction with the photon beam generated by Compton scattering.

The energy spectrum of a photon beam can be directly measured by placing a small detector on the photon beam axis in the LEPS2 experimental building. This measurement provides a smooth spectrum over all the energies in contrast to the indirect measurement by the tagger, which can only determine the energies higher than 1.26 GeV and returns digitized values corresponding to the individual scintillating fiber channels. Figure 10 shows photon-beam energy spectra obtained by using a SF5 lead-glass counter [41, 42] in the LEPS2 experimental building. The dimensions of the lead-glass counter are  $150 \times 150 \text{ mm}^2$  in area and 300 mm in length so as to catch an electromagnetic shower without leak-

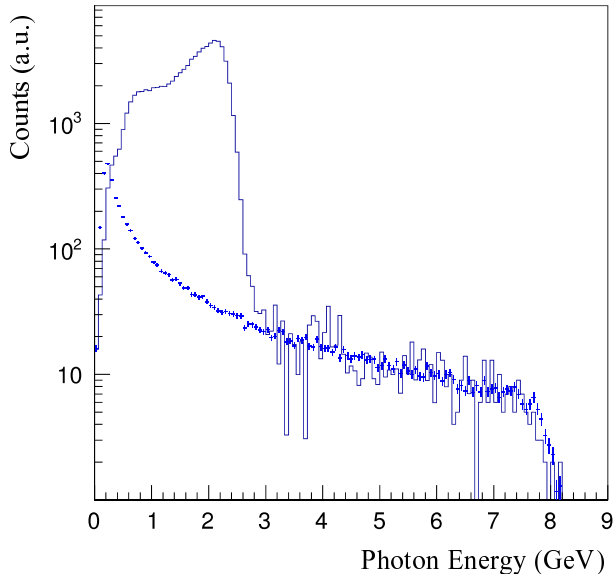


Figure 10: Photon-beam energy spectra measured by a lead-glass counter. Two spectra when laser injection is turned on (dark-blue histogram) and off (blue crosses) are overlaid.

age. Data was taken by self-triggers of the lead-glass counter. The photon beam intensity was intentionally lowered down to a tagger trigger rate of  $0.7 \times 10^6 \text{ s}^{-1}$  for suppressing pile-up signals. The two spectra with and without laser injection were normalized by a gas-bremsstrahlung component in the energy range above 5 GeV. A small contribution from pile-up signals, appearing mainly in the energy range below 5 GeV, was subtracted by using a spectrum for events where multiple hits were clearly found in a short time range. In the case that laser light is injected into the storage ring, a component of  $\gamma$  rays produced by Compton scattering is observed with a strength that is roughly two orders of magnitude higher than that by bremsstrahlung. It is also seen that the energy region lower than around 0.5 GeV is cut off by the effect of the lead collimator with a diameter of 7 mm.

A photon beam energy measured for each event by using the tagger is fluctuated around a true value with a finite resolution. By shifting the relative positions of the two layers of scintillating fibers, recoil electrons can be detected with an accuracy of each

0.5 mm, which corresponds to a tagger energy resolution of 4.3 MeV, as described in Sec. 6. However, the actual energy resolution has been evaluated to be 12.1 MeV by comparing a photon beam energy measured by the tagger with an independent value predicted from the kinematic fit for a coincident photoproduction reaction. This resolution was confirmed by an alternative method where a complementary error function was fitted to the Compton edge of the energy spectrum measured by the tagger for evaluating a convolved uncertainty. The photon-beam energy resolution worse than the detector resolution of the tagger is caused by the energy spread (0.11%) and angular divergence (8 and  $0.7 \mu\text{rad}$  in the horizontal and vertical directions, respectively) of the stored electron beam, resulting in the fluctuation of recoil-electron momenta and angles. If these effects are taken into account as the uncertainty of tagger hit positions, a simulated energy resolution reproduces the measured value.

Figure 11 shows photon beam profiles measured by using a beam profile monitor (BPM) in the LEPS2 experimental building [43]. The BPM is fabricated by arranging 25 scintillating fibers of 3-mm square each to make a plane sensitive to charged tracks and then by stacking two planes whose fiber directions are orthogonal to each other. A signal from each fiber is read out by a Multi-Pixel Photon Counter (MPPC) to identify a combination of vertical and horizontal fiber channels which an electron and positron pair created at a converter have passed through. The  $\sigma$  of observed photon beam spread is about 3 mm for the energy region higher than 1.6 GeV. It is consistent with the beam spread calculated by convolving the electron beam divergence with the kinematical angular broadening of laser Compton scattering, as shown in Fig. 1, and taking into account the distance of photon beam propagation to the LEPS2 experimental building.

Because the electron beam divergence of the LEPS2 beamline is much better than that of the LEPS beamline, it can be observed that a beam size changes depending on the photon beam energy, as expected from the kinematics of laser Compton scattering. (Compare Fig. 11 (a) and (b), or (c) and (d).) It is also seen that the major-axis direction of the

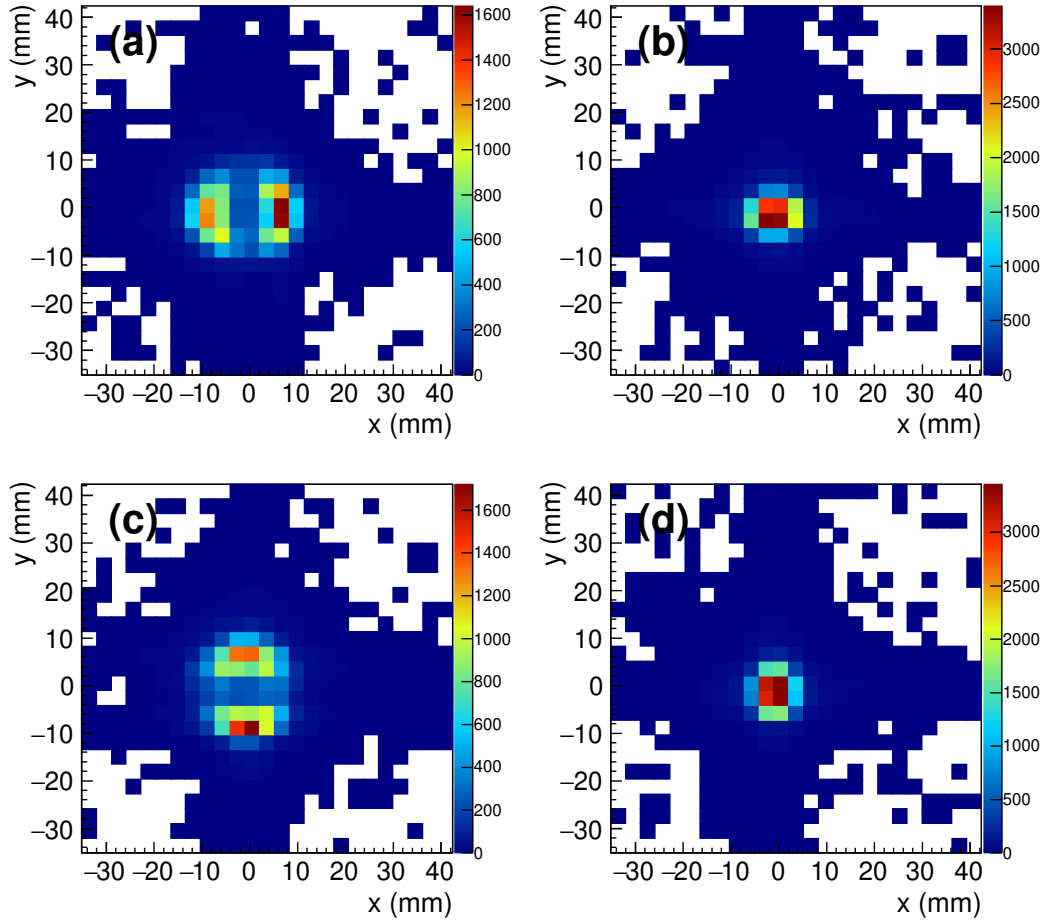


Figure 11: Photon beam profiles when the direction of linear polarization is vertical ((a) and (b)) and horizontal ((c) and (d)). The left panels ((a) and (c)) are plotted for the photon beam energy range of 0.7–1.6 GeV, while the right panels ((b) and (d)) for that of 1.6–2.4 GeV.

beam profile changes by 90 degrees depending on the direction of linear polarization. (Compare Fig. 11 (a) and (c).) This means that radiation tends to occur at the angles perpendicular to the linear polarization direction or the direction of the electric field oscillation. This behavior agrees with a simulation result based on the formula by QED [44].

## 8. Summary and future prospects

The second laser-Compton-scattering facility, called the LEPS2 beamline, has been constructed at SPring-8, which is a storage ring of 8-GeV electrons. A linearly polarized photon beam is available in a tagged energy range of 1.3–2.4 GeV by the injection of UV laser light with a wavelength of 355 nm, and hadron photoproduction experiments are already underway. The photon beam energy can be determined for each event by measuring the momentum of a recoil electron at the tagger, where the lower limit of the tagged energy region is lowered to 1.3 GeV from that of the LEPS beamline (1.5 GeV). The photon-beam energy resolution is estimated to be 12.1 MeV. Since the electron beam divergence is small at the long straight section of the storage ring used by the LEPS2 beamline, the photon beam generated by Compton scattering does not spread and can be extracted over a long distance. Therefore, the LEPS2 experimental building independent of the building housing the storage ring has been constructed at a location about 130 m away from the Compton scattering point. The construction of the LEPS2 experimental building has enabled the installation of two large detector systems covering almost all the solid angles. For enhancing the intensity of the photon beam reaching the LEPS2 experimental building, the LEPS2 beamline is designed to allow the simultaneous injection of four laser beams at a maximum and increase the transmittance of the generated photon beam. The internal diameters of ultra-high vacuum chambers connected to the storage ring are expanded so that multiple laser beams can pass through. The shape of the first mirror used for laser injection in a vacuum is designed to avoid direct hits of  $X$  rays by synchrotron radiation and  $\gamma$  rays by laser Compton scattering. The photon beam intensity is evaluated by counting the number

of tagger trigger signals. In the LEPS beamline, the tagger trigger counts were largely contaminated by the influence of electromagnetic shower produced at the internal structure of the vacuum chamber having a window for the tagger. Thus, the corresponding chamber in the LEPS2 beamline has been improved so as to reduce such contamination by removing a wall structure which is hit by high-momentum recoil electrons. The maximum intensity of the photon beam that can be used for hadron photoproduction experiments in the LEPS2 experimental building was  $2.3 \times 10^6 \text{ s}^{-1}$ . By combining the photon beam having high intensity and linear polarization with the detector systems having high resolutions and acceptances, we can systematically study the nature of hadrons.

In the near future, we will introduce the latest type of pulsed lasers [45] in order to further increase the photon beam intensity. Recently, Spectronics Corp. has released a pulsed UV laser (355-nm wavelength) capable of synchronous output by an external signal. It is now possible to inject pulsed laser light at the timing synchronized with an electron beam bunch in the storage ring [46, 47]. In contrast to the case of continuous wave (CW) or pseudo-CW laser light, the incident laser pulse can efficiently collide with electrons at the focal point without wasting any laser power. Thus, significant improvement of the photon beam intensity is expected. In the LEPS2 beamline, a finite incident angle of laser light is inevitably needed due to the simultaneous injection of multiple laser beams. The decrease of a photon beam intensity due to the crossing of the electron and laser beam axes around the laser focus can be minimized in the case of using a pulsed laser because their scattering positions are always fixed at a single point. We have conducted operational tests of the pulsed UV laser at the LEPS beamline, and the results will be discussed in a separate paper with a detailed description of the method.

This new laser technology is available not only for the UV wavelength that is currently used but also for deep-UV wavelengths that can provide higher energy photon beams. In particular, the output powers of pulsed deep-UV lasers have been much improved. For the wavelength of 266 nm, a new pulsed laser developed by Spectronics Corp. has achieved an out-

put power of about 20 W. This value is an order of magnitude higher than the output power of existing deep-UV lasers and rather comparable to that of high-power UV lasers. In addition, a pulsed deep-UV laser whose output power is in the watt class for a wavelength of 213 nm has become a reality. If it is used at SPring-8, the maximum energy of a photon beam reaches 3.3 GeV.

We would like to thank the staff at SPring-8 for supporting the construction and commissioning of the LEPS2 beamline and giving excellent experimental conditions. We also thank Y. Ishizawa for supporting the maintenance of our interlock system. We appreciate the RIKEN for financially supporting the construction of the LEPS2 experimental building. We are grateful to the technical staff at ELPH, Tohoku University for supporting the production of electronic circuits for the tagger and a beam profile monitor. The use of the BL31LEP of SPring-8 (the LEPS2 beamline) has been approved by the Japan Synchrotron Radiation Institute (JASRI) as a contract beamline (Proposal Nos. BL31LEP/6101 and 6102). This research is supported in part by the Ministry of Education, Science, Sports and Culture of Japan.

## References

- [1] N. Muramatsu, Y. Kon, S. Daté, Y. Ohashi, et al., Development of high intensity laser-electron photon beams up to 2.9 GeV at the SPring-8 LEPS beamline, *Nucl. Instrum. Methods A* 737 (2014) 184–194.
- [2] N. Muramatsu, GeV Photon Beams for Nuclear/Particle Physics, arXiv:1201.4094 (2012).
- [3] O. Bartalini et al., Measurement of  $\pi^0$  photoproduction on the proton from 550 to 1500 MeV at GRAAL, *Eur. Phys. J. A.* 26 (2005) 399–419.
- [4] G. Blanpied et al. (The LEGS Collaboration),  $N \rightarrow \Delta$  transition and proton polarizabilities from measurements of  $p(\vec{\gamma}, \gamma)$ ,  $p(\vec{\gamma}, \pi^0)$  and  $p(\vec{\gamma}, \pi^+)$ , *Phys. Rev. C* 64 (2001) 025203.
- [5] D.I. Sober, et al., The bremsstrahlung tagged photon beam in Hall B at JLab, *Nucl. Instrum. Methods A* 440 (2000) 263–284.
- [6] D. Elsner, et al. (The CBELSA/TAPS Collaboration), Linearly polarised photon beams at ELSA and measurement of the beam asymmetry in  $\pi^0$  photoproduction off the proton, *Eur. Phys. J. A* 39 (2009) 373–381.
- [7] A. Thomas, The Gerasimov-Drell-Hearn sum rule at MAMI, *Eur. Phys. J. A* 28 (2006), s01, 161–171.
- [8] H. Yamazaki, et al., The 1.2 GeV photon tagging system at LNS-Tohoku, *Nucl. Instrum. Methods A* 536 (2005) 70–78.
- [9] T. Ishikawa, et al., The second GeV tagged photon beamline at ELPH, *Nucl. Instrum. Methods A* 622 (2010) 1–10.
- [10] E. Feenberg and H. Primakoff, Interaction of Cosmic-Ray Primaries with Sunlight and Starlight, *Phys. Rev.* 73 (1948) 449–469.
- [11] R.H. Milburn, Electron Scattering by an Intense Polarized Photon Field, *Phys. Rev. Lett.* 10 (1963) 75–77.
- [12] F.R. Arutyunyan and V.A. Tumanian, The Compton Effect on Relativistic Electrons and the Possibility of Obtaining High Energy Beams, *Phys. Lett.* 4 (1963) 176–178.
- [13] K. Horikawa, et al., Neutron angular distribution in  $(\gamma, n)$  reactions with linearly polarized  $\gamma$ -ray beam generated by laser Compton scattering, *Phys. Lett. B* 737 (2014) 109–113.
- [14] T. Maruyama, T. Hayakawa, and T. Kajino, Compton Scattering of  $\gamma$ -Ray Vortex with Laguerre Gaussian Wave Function, *Sci. Rep.* 9 (2019) 51.
- [15] H. Ohgaki, et al., Nondestructive Inspection System for Special Nuclear Material Using Inertial Electrostatic Confinement Fusion Neutrons and Laser Compton Scattering Gamma-Rays, *IEEE Trans. Nucl. Sci.* 64 (2017) 1635–1640.

- [16] E. Hecht, Optics 5th ed., Pearson Education, Inc. (2016).
- [17] A. D'Angelo et al., Generation of Compton backscattering  $\gamma$ -ray beams, Nucl. Instrum. and Methods A 455 (2000) 1–6.
- [18] T. Nakano, et al., Multi-GeV laser-electron photon project at SPring-8, Nucl. Phys. A 684 (2001) 71c–79c.
- [19] U. Timm, Coherent bremsstrahlung of electrons in crystals, Fortschr. Phys. 17 (1969) 765–808.
- [20] S. Adhikari, et al., The GlueX beamline and detector, Nucl. Instrum. Methods A 987 (2021) 164807.
- [21] H. Olsen and L.C. Maximon, Photon and Electron Polarization in High-Energy Bremsstrahlung and Pair Production with Screening, Phys. Rev. 114 (1959) 887.
- [22] H. Tanaka, et al., Stable top-up operation at SPring-8, J. Synchrotron Radiat. 13 (2006) 378–391.
- [23] N. Muramatsu, First Beam Observation and Near Future Plans at SPring-8 LEPS2 Experiment, arXiv:1307.6411 (2013); ELPH Report 2044-13 (2013).
- [24] M. Sumihama, et al. (LEPS Collaboration), The  $\vec{\gamma}p \rightarrow K^+\Lambda$  and  $\vec{\gamma}p \rightarrow K^+\Sigma^0$  reactions at forward angles with photon energies from 1.5 to 2.4 GeV, Phys. Rev. C 73 (2006) 035214.
- [25] Y. Shimosaki, et al., New Optics with Emittance Reduction at the SPring-8 Storage Ring, Proceedings of IPAC2013 (2013) 133–135.
- [26] <https://www.coherent.com/lasers/laser/paladin-advanced-355>
- [27] T. Yorita, et al., Production of Intense High Energy Gamma Beam for LEPS2 Project at SPring-8, Proceedings of IPAC2013 (2013) 2162–2164.
- [28] Y. Asano, S. Miyamoto, and LEPS-II collaboration, Shielding Design of Laser Electron Photon Beamlines at SPring-8, Progress in Nuclear Science and Technology Vol. 4 (2014) 252–256.
- [29] T. Ishikawa, et al., Testing a prototype BGO calorimeter with 100–800 MeV positron beams, Nucl. Instrum. Methods A 837 (2016) 109–122.
- [30] N. Muramatsu, et al. (LEPS2/BGOegg Collaboration), Measurement of neutral pion photoproduction off the proton with the large acceptance electromagnetic calorimeter BGOegg, Phys. Rev. C 100 (2019) 055202.
- [31] N. Tomida, N. Muramatsu, M. Niiyama, et al. (LEPS2/BGOegg Collaboration), Search for  $\eta'$  Bound Nuclei in the  $^{12}\text{C}(\gamma, p)$  Reaction with Simultaneous Detection of Decay Products, Phys. Rev. Lett. 124 (2020) 202501.
- [32] N. Muramatsu, et al. (LEPS2/BGOegg Collaboration), Differential cross sections, photon beam asymmetries, and spin density matrix elements of  $\omega$  photoproduction off the proton at  $E_\gamma = 1.3\text{--}2.4$  GeV, Phys. Rev. C 102 (2020) 025201.
- [33] M.S. Atiya, et al., A detector to search for  $K^+ \rightarrow \pi^+\nu\bar{\nu}$ , Nucl. Instrum. Methods A 321 (1992) 129–151.
- [34] S.Y. Ryu and the LEPS2 Collaboration, Current Status of the LEPS2 Experiment and Commissioning of the Solenoid Spectrometer, AIP Conf. Proc. 2249 (2020) 030024.
- [35] T. Nakano, et al., Evidence for a Narrow  $S = +1$  Baryon Resonance in Photoproduction from the Neutron, Phys. Rev. Lett. 91 (2003) 012002.
- [36] T. Nakano, N. Muramatsu, et al., Evidence for the  $\Theta^+$  in the  $\gamma d \rightarrow K^+K^-pn$  reaction by detecting  $K^+K^-$  pairs, Phys. Rev. C 79 (2009) 025210.
- [37] T. Hyodo and M. Niiyama, QCD and the strange baryon spectrum, Prog. Part. Nucl. Phys. 120 (2021) 103868.

- [38] M. Mai, Review of the  $\Lambda(1405)$  A curious case of a strangeness resonance, *Eur. Phys. J. Spec. Top.* 230 (2021) 1593–1607.
- [39] T. Nakamura, et al., Filling of High Current Singlet and Train of Low Bunch Current in SPring-8 Storage Ring, *Proceedings of EPAC08 (2008)* 3284–3286.
- [40] H. Saito, Development of the photon-beam transmittance measurement system at the LEPS2 beamline, Master’s Thesis, Tohoku Univ. (2021).
- [41] A. Ando, S. Inaba, T. Inagaki, K. Takamatsu, T. Tsuru, Y. Inagaki, Electron Beam Test of the Active Converter Device, *KEK Reports* 79-21 (1979).
- [42] T. Ishikawa, et al., The FOREST detector for meson photoproduction experiments at ELPH, *Nucl. Instrum. Methods A* 832 (2016) 108–143.
- [43] R. Shirai, Measurement of the gamma beam profile by newly developed beam profile monitor for missing resonance search experiment, Master’s Thesis, Tohoku Univ. (2018).
- [44] C. Sun and Y.K. Wu, Theoretical and simulation studies of characteristics of a Compton light source, *Phys. Rev. ST Accel. Beams* 14 (2011) 044701.
- [45] <https://www.spectronix-laser.com/>
- [46] H. Katsuragawa, Installation of a pulse laser at the LEPS beamline, RCNP Annual Report 2020, Osaka Univ. (2021) “Highlights” section.
- [47] N. Muramatsu, H. Katsuragawa, T. Nakano, Y. Ohashi, S. Date, and Y. Orii, Pulse laser test for the backward Compton scattering at the SPring-8 LEPS beamline, *ELPH Annual Report 2016 (2017)* 66–67.